

## Antioxidant Enzymes Mediate Survival of Breast Cancer Cells Deprived of Extracellular Matrix

Calli A. Davison<sup>1</sup>, Sienna M. Durbin<sup>1</sup>, Matthew R. Thau<sup>1</sup>, Victoria R. Zellmer<sup>1</sup>, Sarah E. Chapman<sup>2</sup>, Justin Diener<sup>2</sup>, Connor Wathen<sup>2</sup>, W. Matthew Leevy<sup>2,3</sup>, and Zachary T. Schafer<sup>1</sup>

### Abstract

Metastasis by cancer cells relies upon the acquisition of the ability to evade anoikis, a cell death process elicited by detachment from extracellular matrix (ECM). The molecular mechanisms that ECM-detached cancer cells use to survive are not understood. Striking increases in reactive oxygen species (ROS) occur in ECM-detached mammary epithelial cells, threatening cell viability by inhibiting ATP production, suggesting that ROS must be neutralized if cells are to survive ECM-detachment. Here, we report the discovery of a prominent role for antioxidant enzymes, including catalase and superoxide dismutase, in facilitating the survival of breast cancer cells after ECM-detachment. Enhanced expression of antioxidant enzymes in nonmalignant mammary epithelial cells detached from ECM resulted in ATP elevation and survival in the luminal space of mammary acini. Conversely, silencing antioxidant enzyme expression in multiple breast cancer cell lines caused ATP reduction and compromised anchorage-independent growth. Notably, antioxidant enzyme-deficient cancer cells were compromised in their ability to form tumors in mice. In aggregate, our results reveal a vital role for antioxidant enzyme activity in maintaining metabolic activity and anchorage-independent growth in breast cancer cells. Furthermore, these findings imply that eliminating antioxidant enzyme activity may be an effective strategy to enhance susceptibility to cell death in cancer cells that may otherwise survive ECM-detachment. *Cancer Res*; 73(12); 3704–15. ©2013 AACR.

### Introduction

Mammary epithelial cells require attachment to the extracellular matrix (ECM) for survival, and ECM-detachment results in the induction of a caspase-mediated cell death program known as anoikis (1–3). As such, tumor cells require resistance to anoikis to survive during cancer progression (4, 5). The ability to evade anoikis is critically important during the metastatic cascade, as cancer cells are forced to survive in the absence of ECM-attachment while in the blood or lymphatic vessels. Therefore, a better understanding of how cancer cells survive in the absence of ECM-attachment could ultimately lead to the development of novel therapeutic approaches to inhibit tumor progression and metastasis.

Interestingly, previous research has revealed that inhibition of anoikis is not sufficient to promote the long-term survival of

ECM-detached cells (6). Multiple anoikis-independent pathways have been discovered to contribute to cell death following ECM-detachment (7–9). We have previously shown that an energy deficiency (diminished ATP levels) caused by ECM-detachment can compromise the viability of these cells independent of the induction of anoikis (10). We discovered that oncogenic signaling can rectify metabolic defects in ECM-detached cells by enhancing glucose uptake, promoting flux through the pentose phosphate pathway (PPP), stimulating NADPH generation, and the subsequent elimination of ECM detachment-induced reactive oxygen species (ROS). In addition, we found that the neutralization of ROS is sufficient to elevate ATP levels and to promote the survival of ECM-detached cells independently of any changes in glucose uptake (10). Together, these data unmask detachment-induced ROS as a critical barrier to the long-term survival of ECM-detached cells and presumably to the successful metastasis of tumor cells (11).

The discovery of this novel obstruction to the viability of ECM-detached cells suggests that metastatic cancer cells have developed mechanisms to eliminate detachment-induced ROS. Typically, eukaryotic cells depend on multiple antioxidant enzymes to remove excess quantities of ROS. Catalase is a ubiquitous oxidoreductase that neutralizes hydrogen peroxide by converting it into water and molecular oxygen (12). Likewise, superoxide dismutases, a family of 3 antioxidant enzymes (SOD1, SOD2, and SOD3), are responsible for the elimination of superoxide (13). These enzymes vary in their localization as

**Authors' Affiliations:** <sup>1</sup>Department of Biological Sciences; <sup>2</sup>Notre Dame Integrated Imaging Facility; and <sup>3</sup>Department of Chemistry and Biochemistry, University of Notre Dame, Notre Dame, Indiana

**Note:** Supplementary data for this article are available at Cancer Research Online (<http://cancerres.aacrjournals.org/>).

**Corresponding Author:** Zachary T. Schafer, Department of Biological Sciences, University of Notre Dame, 222 Galvin Life Science Center, Notre Dame, IN 46556. Phone: 574-631-0875; Fax: 574-631-7413; E-mail: zschafe1@nd.edu

doi: 10.1158/0008-5472.CAN-12-2482

©2013 American Association for Cancer Research.

CuZn-SOD (SOD1) is expressed in the cytoplasm, nuclear compartments, and lysosomes of cells, whereas Mn-SOD (SOD2) specifically localizes to the mitochondria.

Given the important role of these enzymes in modulating ROS, it is possible that during periods of ECM-detachment, the activity of antioxidant enzymes is necessary to maintain robust ATP production and promote survival. Multiple lines of evidence suggest a role for the activity of antioxidant enzymes in tumor progression. Immunohistochemical analyses of antioxidant enzyme expression in breast cancer tissue have revealed that catalase, SOD1, and SOD2 have amplified expression in tumor tissue when compared with adjacent benign tissue (14). More recently, SOD1 was discovered to be the molecular target of a potent compound that inhibits the growth of lung adenocarcinoma cell lines (15), suggesting that the pharmacologic inhibition of antioxidant enzymes could be an effective strategy to impede tumor progression.

In this study, we assess the role of antioxidant enzymes in mediating the survival of ECM-detached cells and the importance of antioxidant enzymes to the anchorage-independent growth of cancer cells. We show that the expression of antioxidant enzymes in mammary epithelial cells enhances ATP generation in ECM-detached cells and promotes their survival in the luminal space of mammary acini. Furthermore, we have discovered that the elimination of antioxidant enzyme expression in breast cancer cells limits ATP production in suspension, prohibits vigorous anchorage-independent growth, and reduces lung tumor burden in mouse xenograft assays. In aggregate, these data reveal that antioxidant enzymes are critical for the anchorage-independent survival of breast cancer cells and suggest that antioxidant enzymes may be a viable target for the development of novel chemotherapeutics aimed at eradicating ECM-detached cells.

## Materials and Methods

### Cell culture

MCF-10A cells were cultured as described previously (10). T47D cells [American Type Culture Collection (ATCC)] were cultured in RPMI-1640 media (GIBCO) plus 10% FBS (GIBCO). SKBR3 cells (ATCC) were cultured in McCoy's media (GIBCO) plus 10% FBS. MDA-MB-231 cells (ATCC) were cultured in Dulbecco's Modified Eagle Medium (GIBCO) plus 10% FBS. Penicillin/streptomycin, and plasmocin were added to all cultures.

### ATP assays

For the measure of ATP in detached cells, the ATP Determination Kit (Invitrogen) was used as described previously (10). The data from these assays show representative experiments from at least 3 independent replicates.

### Caspase assays

Caspase activation was measured using the Caspase-Glo 3/7 Assay Kit (Promega). Cells were plated at a density of 13,333 cells per well in 96-well poly-(2-hydroxyethyl methacrylate) (poly-HEMA) coated plates. Caspase activation was measured according to manufacturer's instructions.

### Proliferation and cell death assays

For measuring cell proliferation, 75,000 cells in 1 mL of media were plated per well of a 6-well plate. At 24, 48, and 72 hours, cells were stained with Trypan blue (Invitrogen) and counted using a hemocytometer.

### Western blotting

Cells were lysed in 1% NP40 on ice for 20 minutes. Lysates were spun at  $14,000 \times g$  at  $4^{\circ}\text{C}$  for 30 minutes and normalized using a BCA Assay (Pierce Biotechnology). Lysates were then subjected to SDS-PAGE and transfer/blotting was conducted as previously described (16).

### Glucose uptake assays

Glucose uptake was measured using the Amplex Red Glucose Assay Kit (Invitrogen) as described previously (10). The data shown in the figures show representative experiments from at least 3 independent replicates.

### ROS assays

Cells were plated at a density of 13,333 cells per well in 96-well poly-HEMA-coated plates. After 24 hours, carboxy-  $\text{H}_2$  DCFDA (Invitrogen) or CellROX Green Reagent (Invitrogen) was added to each well at a concentration of  $10 \mu\text{mol/L}$  and mixed vigorously. Fluorescence of both Carboxy-  $\text{H}_2$  DCFDA and CellROX was measured using a plate reader. In some cases, Amplex Red (Invitrogen) was used to measure ROS according to manufacturer's specifications.

### Soft agar assays

Cells were plated in soft agar experiments as described previously (10). In antioxidant compound experiments, the indicated concentration was added at the time of plating and at feedings throughout the duration of the experiment. Colony number was determined as described previously (10). The figures including data from these assays show representative experiments from at least 3 independent replicates.

### Retroviral transduction

The pLNCX-Neo-based retroviral vectors encoding wild-type catalase, and catalase with the signal sequence SKL were used to generate stable cell lines as described previously (10).

### 3D cell culture

To generate acini, cells were grown as described previously (17). Immunofluorescence of acini was conducted as described previously (17). For examination of luminal filling, acini were imaged using confocal microscopy (Nikon A1R) to visualize the center of each structure, and then were scored as described previously (10). The figures including data from these assays show representative experiments from at least 3 independent replicates.

### AlamarBlue assay

Cells were plated at a density of 13,333 cells per well in 96-well poly-HEMA-coated plates. Ten microliters of AlamarBlue reagent (Invitrogen) was added to each well and incubated at  $37^{\circ}\text{C}$  for 1 to 4 hours and fluorescence was measured on a plate reader.

### Fatty acid oxidation assay

Fatty acid oxidation (FAO) was measured in the indicated cells as described previously (10). The figure from these assays shows pooled and normalized data from multiple experiments.

### Short hairpin RNA

Mission (Sigma-Aldrich) short hairpin RNA (shRNA) constructs were used and the PLKO.4 shRNA viruses were produced and used to generate stable knockdowns as described previously (10).

### Mice

Female athymic mice (Foxn1-nu), 5- to 6-week-old were obtained from Harlan Laboratories. We injected  $2 \times 10^6$  MDA-MB-231 cells into the lateral tail vein of 7-week-old female nude mice. Six weeks after injection, the mice were sacrificed and lungs were removed. Lungs were fixed in Bouin's solution for 24 hours and stored in 70% ethanol before analysis. Procedures were evaluated and approved by the University of Notre Dame Institutional Animal Care and Use Committee (Protocol number 13-019).

### Computed tomography imaging and analysis

Computed tomography (CT) images were acquired with a trimodal Albira PET/SPECT/CT imaging system (Carestream Molecular Imaging). Mice were anesthetized with 1.5% isoflurane in an induction box. Mice were placed inside scanner and secured in a tooth bar. A CT scan (110 mm FOV, 45 kVp, 200  $\mu$ A, at 400 projections) was then conducted. The CT scans were reconstructed using the FBP algorithm.

To conduct normal lung density analysis, CT images were first segmented using the PMOD "tools">"external">"segmentation" operation. Segmentation was set to the range  $-550$  to  $-200$  (HU) and the "create a VOI Template/Mask" check box was created to obtain the normal lung density volume. VolView 3.2 (Kitware) was used for image rendering and visualization of CT images. ImageJ v1.44 was used to generate image montages.

### Hematoxylin and eosin staining

Lung tissues were fixed with Bouin's fixative for more than 24 hours. After dehydrating and embedding in paraffin wax, the tissues were cut into 4  $\mu$ m slices. The slices were stained with hematoxylin and eosin. The pathogenesis of lung injury was observed under microscope.

## Results

### Multiple antioxidant compounds enhance ATP production in ECM-detached cells and promote anchorage-independent growth

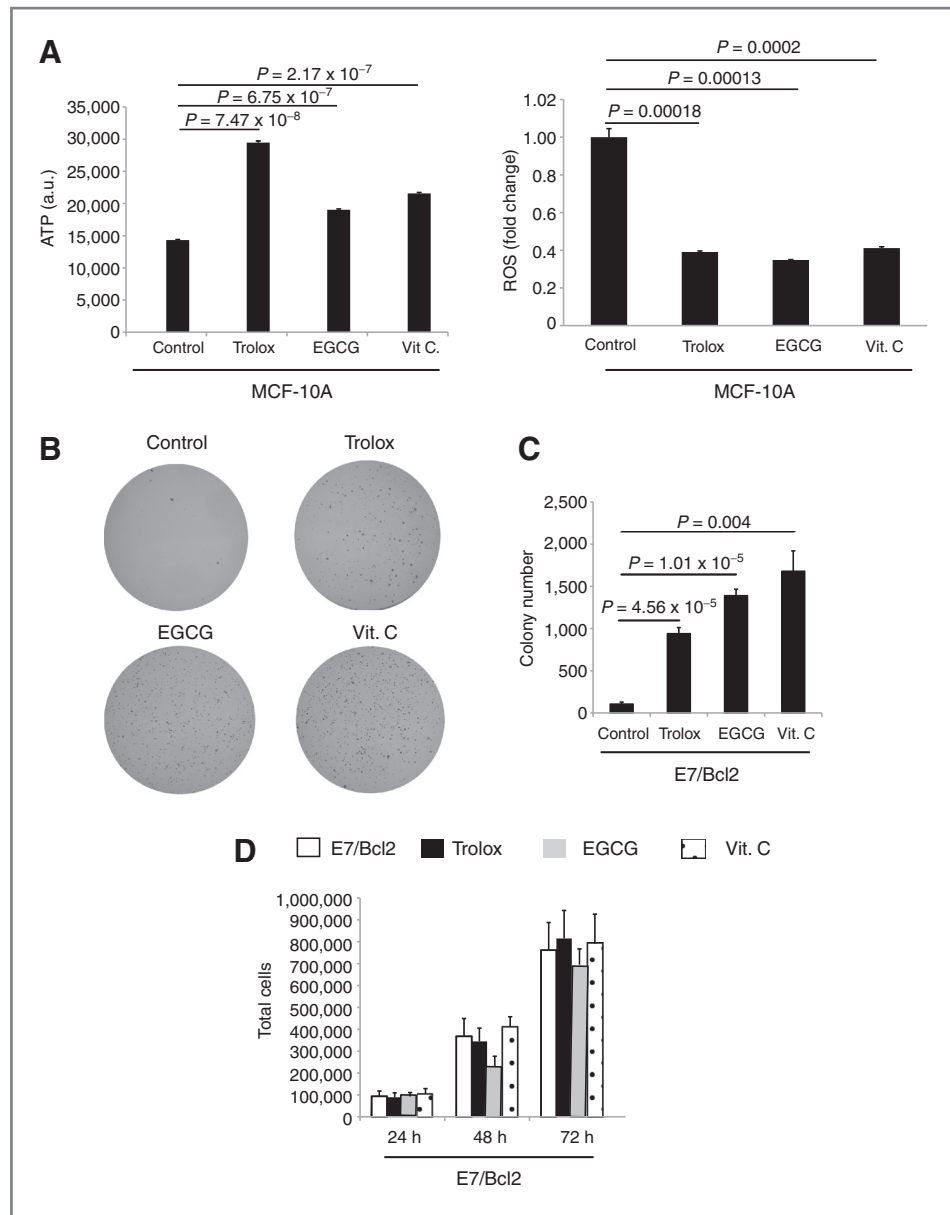
Given that our previous research has revealed that treatment of ECM-detached cells with N-acetyl-L-cysteine (NAC) or Trolox could enhance ATP production and facilitate anchorage independence (10), we investigated the ability of additional antioxidant compounds to promote viability in ECM-detached cells. Using MCF-10A cells, a nonmalignant mammary epithelial cell line, we examined ATP levels in cells cultured on nonadherent plates and treated with the antioxidants Trolox,

epigallocatechin gallate (EGCG), or vitamin C (ascorbic acid). In each case, we were able to effectively diminish ROS levels and detect a statistically significant increase in ATP levels (Fig. 1A). In addition, as noted previously with NAC and Trolox treatment (10), we detected no significant alterations in glucose uptake between untreated and antioxidant treated detached cells (Supplementary Fig. 1). We then sought to understand whether these antioxidant compounds can augment anchorage-independent growth in soft agar assays. To do this, we used MCF-10A cells engineered to express HPV-E7 (to promote proliferation) and Bcl-2 (to block apoptosis) as parental MCF-10A cells lack the capacity to grow in soft agar (10). Treatment of these cultures with Trolox, EGCG, or vitamin C induced a substantial increase in colony number (Fig. 1B and C). In addition, these treatments did not result in any significant alterations to proliferation (Fig. 1D) or cell death (Supplementary Fig. 2) in attached cells, suggesting that the effects of these antioxidants in the soft agar assays are specific to modulation of ATP levels. In addition, we found mixed results with regards to the reversibility of this effect (Supplementary Fig. 3), suggesting that other factors (i.e., compound stability) likely contribute to the stability of this effect. These data reveal that the ability of antioxidant compounds to increase ATP generation and promote anchorage-independent growth is not limited to NAC or Trolox treatment and suggest that multiple ROS-neutralizing mechanisms may be effective in facilitating the survival of ECM-detached cells.

### Overexpression of catalase in mammary epithelial cells promotes ATP generation in ECM-detached cells and promotes luminal filling in mammary acini

Given that antioxidant compounds can rescue the ATP deficiency in ECM-detached cells, we investigated whether increased expression of antioxidant enzymes could similarly affect ATP generation in detached mammary epithelial cells. We engineered cell lines with elevated expression of catalase, an antioxidant enzyme that has been shown to be involved in cell survival in breast cancer cells (18, 19). Given that the distinct localization of catalase to the peroxisome has previously been revealed to enhance its antioxidant activity (20), we expressed diffusely localized (KANL) or peroxisomally targeted (SKL) catalase in MCF-10A cells (Fig. 2A). To investigate whether catalase expression rescues ATP production in ECM-detached cells, we examined cellular ATP levels in 10A-KANL and 10A-SKL cells cultured on nonadherent plates. We detected a substantial increase in ATP levels and achieved a comparable reduction in ROS levels in both 10A-KANL and 10A-SKL cells compared with the 10A control (Fig. 2B and C). These data suggest that catalase does not require specific peroxisomal targeting to promote ATP generation in ECM-detached cells. In addition, the increased ATP levels in detached cells expressing catalase was not due to alterations in glucose uptake in these cells (Supplementary Fig. 4). Previously published data has suggested that the neutralization of ROS in ECM-detached cells enhances ATP levels by promoting FAO (10). When examining FAO efficacy in cells with increased catalase

**Figure 1.** Antioxidant compounds promote ATP production in ECM-detached cells and anchorage-independent growth. **A**, 10A cells were grown in detached conditions and treated with 50  $\mu\text{mol/L}$  of indicated antioxidant compound, and ATP was measured after 24 hours in suspension (left). Error bars represent SD, and *P* values were determined using 2-tailed *t* test. ROS (right) was measured using carboxy- $\text{H}_2\text{DCFDA}$  after 24 hours in suspension. Error bars represent SEM, and *P* values were determined using 2-tailed *t* test. **B** and **C**, 10A-E7/Bcl-2 cells were grown in soft agar for 24 days and were treated with indicated antioxidant compounds every 2 days. Colonies were stained with iodinitrotetrazolium violet and counted using ImageJ. Representative images are shown in **B** and quantitation of colony number is shown in **C**. Error bars represent SD, and *P* values were determined using 2-tailed *t* test. **D**, 10A-E7/Bcl-2 cells were plated in the presence or absence of indicated antioxidant compounds, and cells were counted at the indicated time point. Error bars represent SEM, and *P* values were determined using a 2-tailed *t* test.



expression, we discovered that FAO was significantly augmented (Fig. 2D). Although these data suggest that catalase expression itself may be induced during ECM-detachment or in transformed cells to facilitate cell survival, we did not detect any alterations in catalase expression during ECM-detachment nor when we compared untransformed MCF-10A cells with breast cancer cells (Supplementary Fig. 5). These data suggest that catalase activity becomes critical to ATP production and survival during ECM-detachment when glucose uptake is diminished (10).

We then asked whether the expression of catalase could promote luminal filling in a three-dimensional (3D) model of mammary acini development (21), a more physiologically relevant model as the centrally located cells die due to lack of ECM-attachment (6, 10, 22–25). The acini generated from

10A-KANL and 10A-SKL cells exhibited a dramatic increase in the number of structures scoring as either "mostly filled" or "filled" when compared with control 10A acini (Fig. 2E). Remarkably, the expression of catalase (either KANL or SKL) did not appreciably alter the induction of anoikis (Fig. 2F), suggesting that catalase-mediated induction of luminal filling is not due to anoikis evasion. Interestingly, when examining how catalase expression affects cell viability at earlier time points after ECM-detachment (i.e., 3 hours), we found that catalase expression enhances ATP levels and cell viability (as measured by AlamarBlue reduction) without affecting anoikis (Supplementary Fig. 6). These data lend further credence to the supposition that catalase expression can promote cell viability by stimulating ATP production.



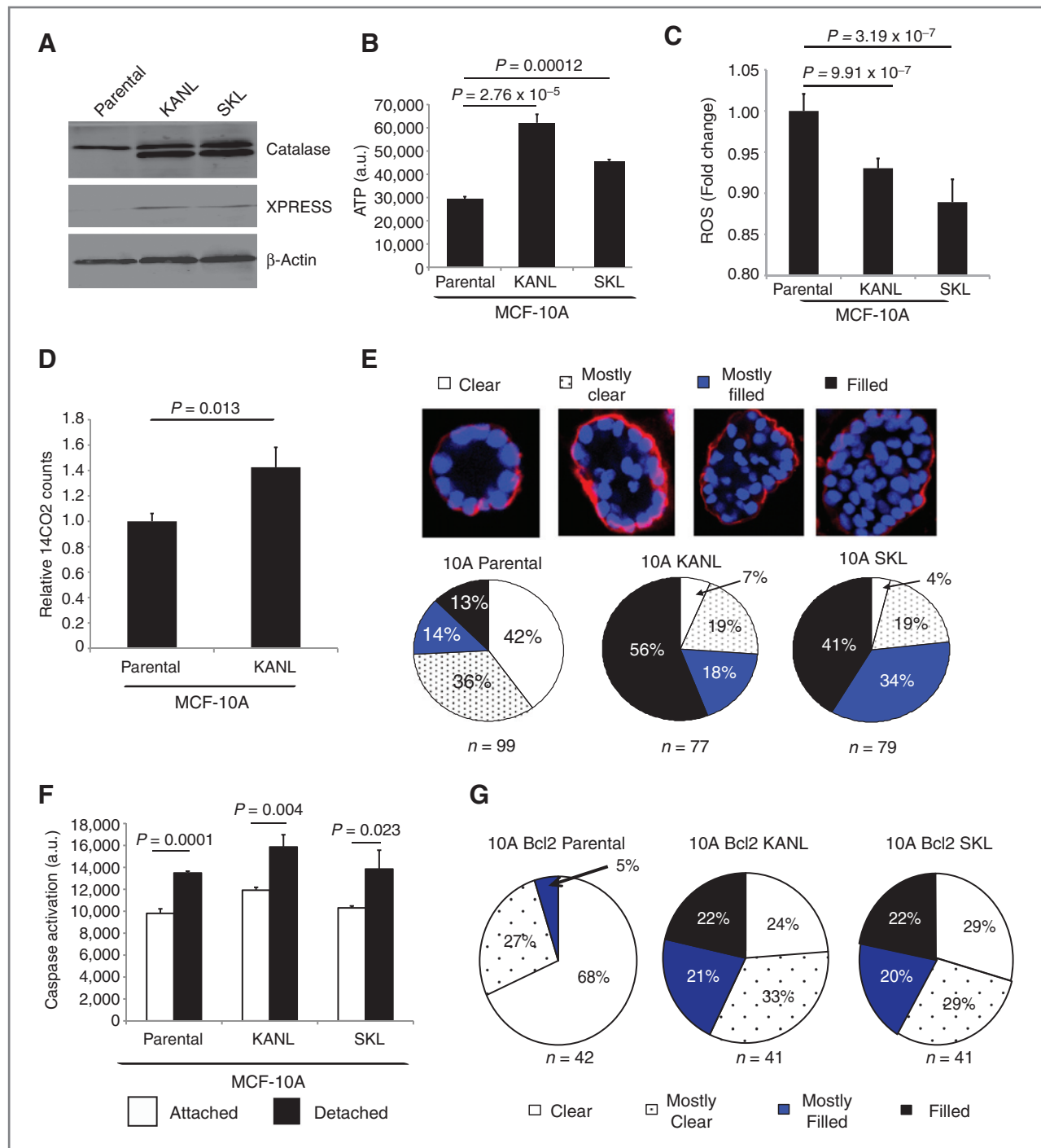


**Figure 2.** Catalase expression elevates ATP levels in ECM-detached cells and facilitates luminal filling in 3D cell culture. **A**, using retroviral transduction, 10A cells were engineered to overexpress XPRESS-tagged catalase (either KANL or SKL). Western blotting for catalase and XPRESS confirmed the success of the transduction.  $\beta$ -actin was used as a loading control. **B**, ATP levels were measured in the indicated cell lines after 24 hours in suspension. Error bars represent SD, and  $P$  values were determined using 2-tailed  $t$  test. **C**, ROS was measured using Amplex Red reagent after 24 hours in suspension. Error bars represent SEM, and  $P$  values were determined using 2-tailed  $t$  test. **D**, FAO levels were measured after 24 hours in suspension. Error bars represent SEM, and  $P$  values were determined using 2-tailed  $t$  test. **E**, mammary acini were generated using the indicated cell lines. At day 14, acini were stained with anti-laminin 5 (red) and the nuclear stain 4',6-diamidino-2-phenylindole (DAPI, blue). Acini were then scored as clear, mostly clear, mostly filled, or filled. Representative images of each of these categories are shown ( $\times 40$ ). **F**, caspase activation was measured in attached and detached conditions in the indicated cell lines 48 hours after plating. Error bars represent SD, and  $P$  values were determined using a 2-tailed  $t$  test. **G**, mammary acini were generated using 10A Bcl-2 cells expressing catalase (KANL or SKL) or 10A Bcl-2 parental cells. At day 14, acini were stained, imaged, and scored as described in **E**.

Downloaded from <http://aacrjournals.org/cancerresearch/article-pdf/73/12/3704/2684589/3704.pdf> by guest on 28 March 2025

To further rule out any connection between catalase and apoptosis, we expressed catalase in 10A cells overexpressing the antiapoptotic protein Bcl-2 (6). Bcl-2-positive acinar structures derived from cells expressing catalase show a similar ability to promote luminal filling as we observe many more "filled" or "mostly filled" structures and a significant loss of "clear" structures (Fig. 2G). These data further show that catalase promotes luminal filling by enhancing ATP generation independently of any effects on anoikis.

### Neutralization of ROS by catalase promotes ATP production by modulating AMPK activation

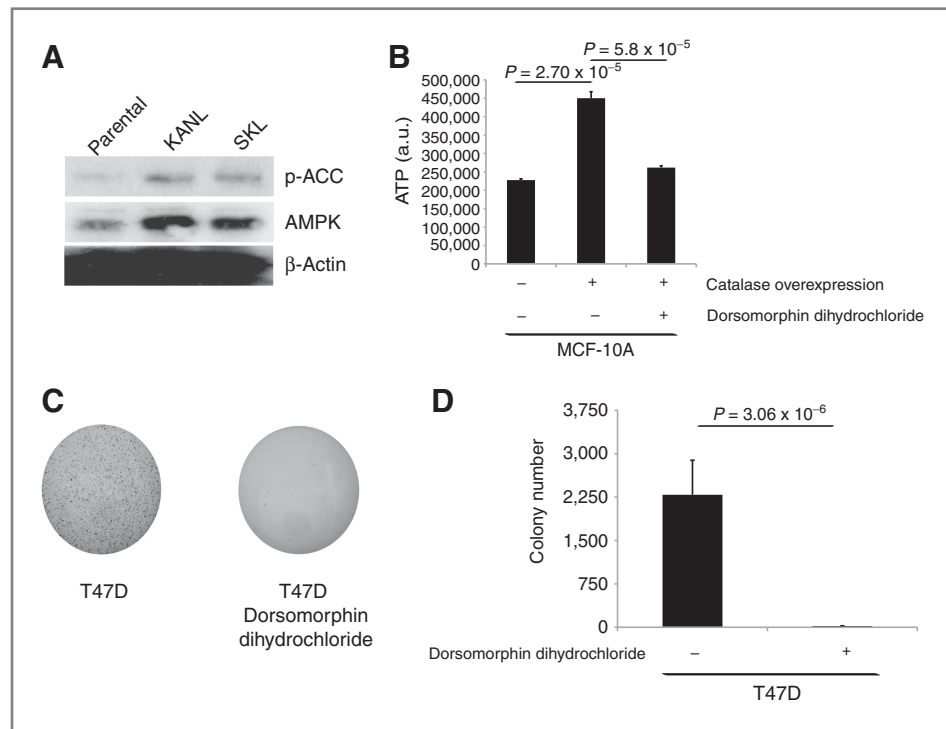
Next we further investigated the molecular mechanism underlying the ability of catalase to improve ATP production in ECM-detached cells. As shown in Fig. 2D, catalase expression promotes FAO in ECM-detached 10A cells. A critical regulator of FAO efficacy is the AMPK pathway. AMPK activation results in the phosphorylation and inhibition of acetyl-CoA carboxylase (ACC), an enzyme that is known to inhibit FAO by producing malonyl-CoA. Given this, we investigated whether catalase expression could alter AMPK activation in ECM-detached cells. Interestingly, we found that total AMPK levels and AMPK activation (as measured by phosphorylation of ACC) were increased in catalase-expressing cells (Fig. 3A). When we inhibited the activation of AMPK in catalase-expressing 10A cells using the inhibitor dorsomorphin dihydrochloride, we found that the catalase-mediated increase in ATP levels was completely abrogated (Fig. 3B). These data suggest that catalase expression enhances AMPK signaling in ECM-detached cells in a fashion that promotes ATP production. To examine whether AMPK activation was critical for anchor-

age-independent growth in breast cancer cells, we treated T47D cells with dorsomorphin dihydrochloride and measured anchorage-independent growth in a soft agar assay. Indeed, AMPK inhibition was sufficient to substantially hinder colony formation in soft agar (Fig. 3C and D). Collectively, these data suggest that catalase expression promotes ATP production and anchorage-independent growth by stimulating the AMPK pathway.

### Catalase is critical for the preservation of ATP production and anchorage-independent growth in ECM-detached invasive breast cancer cells

Given that catalase was sufficient to promote cell viability in nonmalignant ECM-detached mammary epithelial cells, we wondered whether catalase expression was necessary for the survival of invasive breast cancer cells in the absence of ECM-attachment. To address this matter, we used lentiviral-mediated delivery of shRNA to generate an MDA-MB-231 (231) cell line that is deficient in catalase expression (Fig. 4A). Using these cells, we discovered that catalase-deficient 231 cells have a substantial decrease in the production of ATP and increased levels of ROS when detached from the ECM (Fig. 4B and C). This ATP deficit can be rescued through treatment with Trolox (Fig. 4B) or through the reexpression of catalase (Supplementary Fig. 7). In addition, these alterations in ATP levels are not a result of modulations in glucose uptake as no significant changes in glucose uptake are observed when catalase is eliminated (Supplementary Fig. 8). Furthermore, catalase knockdown in 231 cells substantially abrogated anchorage-independent growth (Fig. 4D and E). Anchorage-independent growth could be rescued in catalase-deficient 231 cells through

**Figure 3.** Neutralization of ROS by catalase promotes ATP production by modulating AMPK activation in detached MCF-10A and T47D cells. **A**, MCF-10A cells were grown 24 hours in suspension and total AMPK levels and activated AMPK (phospho-ACC) levels were measured by Western blotting.  $\beta$ -actin was used as a loading control. **B**, MCF-10A cells (parental or overexpressing catalase) were grown in suspension in the presence or absence of 20  $\mu$ mol/L dorsomorphin dihydrochloride (AMPK inhibitor), and ATP levels were measured after 24 hours. **C** and **D**, T47D cells were grown in soft agar for 18 days and were treated with AMPK inhibitor (20  $\mu$ mol/L) every 2 days. Colonies were stained with INT-violet and counted using ImageJ. Representative images are shown in **C** and quantitation of colony number is shown in **D**. All error bars represent SD, and all *P* values were determined using a 2-tailed *t* test.



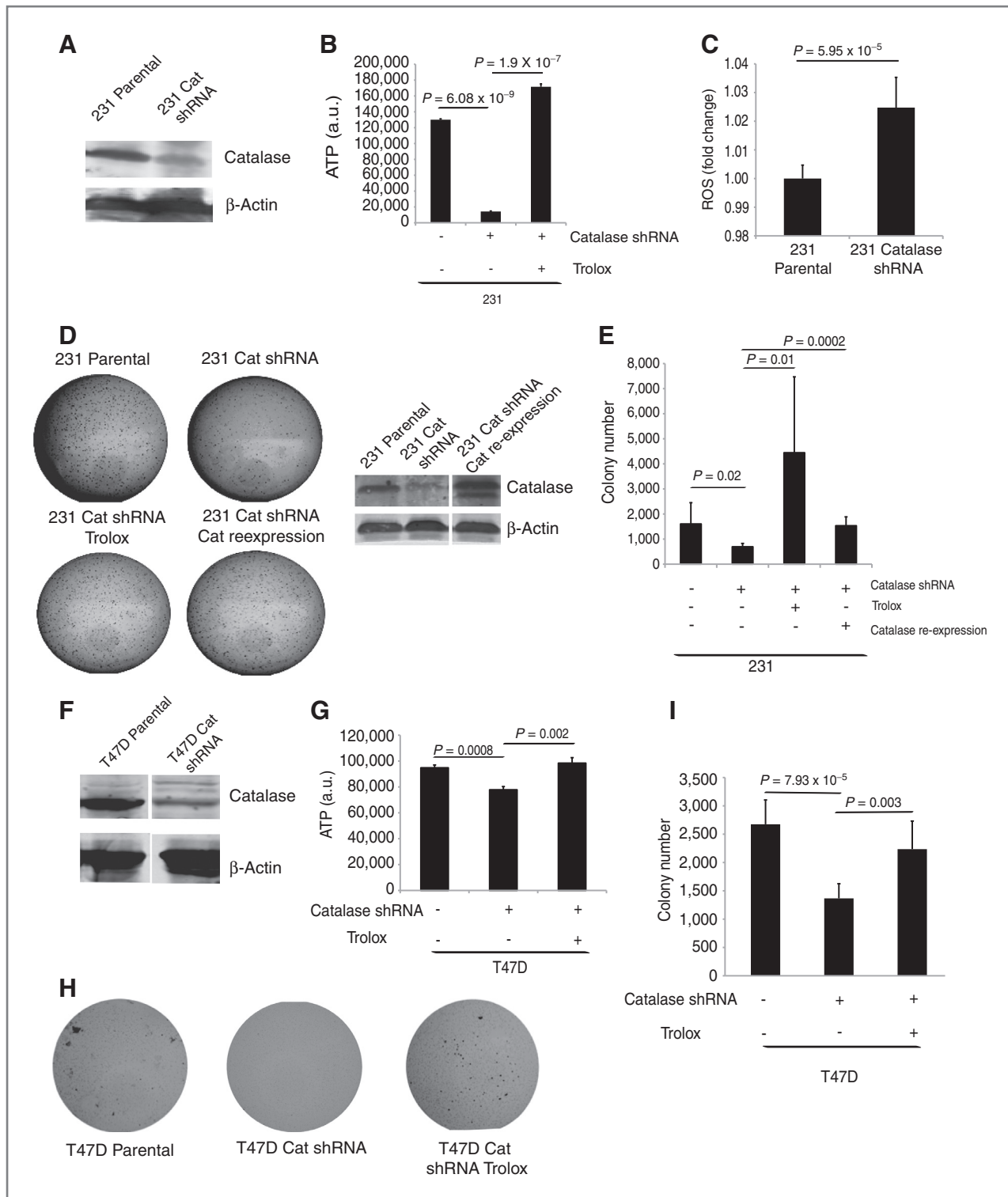


**Figure 4.** Catalase is critical for ATP generation and anchorage-independent growth in MDA-MB-231 cells and T47D cells. **A**, using lentiviral transduction of shRNA, catalase expression was reduced in MDA-MB-231 (231) cells. Immunoblotting for catalase and  $\beta$ -actin (loading control) confirms the success of the transduction. **B**, ATP levels were measured under the indicated conditions after 24 hours of growth in suspension. Trolox treatment was at 50  $\mu$ mol/L. Error bars represent SD, and  $P$  values were determined using a 2-tailed  $t$  test. **C**, ROS levels of indicated cells were measured after 24 hours in suspension using CellROX reagent. Error bars represent SEM, and the  $P$  value was determined by a 2-tailed  $t$  test. **D** and **E**, catalase was reexpressed in the 231 catalase shRNA cells using retroviral transduction. Western blotting for catalase and  $\beta$ -actin (loading control) confirms the success of the transduction (**D**). The indicated cells were grown in soft agar for 24 days and stained with INT-violet and counted using ImageJ. Trolox treatment was at 50  $\mu$ mol/L and applied every 2 days.

Trolox treatment or catalase reexpression (Fig. 4D and E), confirming that the loss of anchorage-independent growth in 231 cells following catalase elimination is due to alterations in oxidative stress. While a number of factors (e.g. proliferation, apoptosis) can alter anchorage-independent growth in soft agar assays, catalase-deficient 231 cells display no marked changes in proliferative capacity (Supplementary Fig. 9) or cell death (Supplementary Fig. 10) compared with control 231 cells. Thus, these data suggest that anchorage-independent growth is inhibited in catalase-deficient invasive breast cancer cells due to ROS-mediated alterations in metabolism.

To investigate whether these data are reproducible in other breast cancer cell lines, we generated catalase-deficient T47D cells (Fig. 4F). Like 231 cells, catalase-deficient T47D cells displayed a significant loss in ATP levels when detached from the ECM that could subsequently be rescued by Trolox treatment (Fig. 4G). These alterations in ATP levels were independent of any changes in glucose uptake (Supplementary Fig. 11). When we examined the ability of these cells to grow in an anchorage-independent fashion, we found that the elimination of catalase dramatically reduced colony formation in a soft agar assay (Fig. 4H and I). The loss of growth in soft agar assays induced by catalase loss could be efficiently rescued through Trolox treatment (Fig. 4H and I). These changes in anchorage-independent growth were not a result of enhanced proliferative capacity (Supplementary Fig. 12) or diminished viability (Supplementary Fig. 13) in attached cells. These data collectively suggest that breast cancer cells rely on catalase to reduce oxidative stress when detached from the ECM.

#### **The elimination of other enzymes involved in reducing oxidative stress in breast cancer cells results in compromised ATP production and diminished anchorage-independent growth**

Given the data above, we postulated that other antioxidant enzymes may provide similar support to ECM-detached cells. To investigate this hypothesis, we engineered T47D cells that are stably deficient in SOD2 (Fig. 5A). Indeed, the loss of SOD2 in ECM-detached T47D cells resulted in a significant reduction of ATP levels (Fig. 5B) that is independent of any alterations in glucose uptake (Supplementary Fig. 14). Furthermore, the reduction of SOD2 expression in T47D cells caused a substantial inhibition of anchorage-independent growth (Fig. 5C and D). Despite these substantial changes, we were unable to detect any alterations in proliferation (Supplementary Fig. 15) or cell viability (in attached cells; Supplementary Fig. 16) when SOD2 expression was reduced. In addition, shRNA-mediated reduction of SOD1 or Nrf2 (a transcription factor that promotes antiox-

idant enzyme expression) in T47D cells resulted in a similar loss of ATP levels (Supplementary Figs. 17 and 18) and a comparable reduction in anchorage-independent growth (Fig. 5E and F). As described above, ErbB2 expression has previously been shown to promote ATP generation in ECM-detached cells through a mechanism involving the promotion of PPP flux and the reduction of ROS (10). However, even in breast cancer cells that overexpress ErbB2 (i.e., SKBR3 cells), the elimination of antioxidant enzymes like SOD2 is sufficient to significantly diminish ATP levels in ECM-detached cells (Supplementary Fig. 19). Collectively, these data reveal that breast cancer cells can rely on the activity of the antioxidant enzyme program to promote anchorage-independent growth.

#### **The activity of antioxidant enzymes is critical for tumor formation *in vivo***

We were interested in determining whether the reduction of antioxidant enzyme activity would also affect tumor formation *in vivo*. To address this question, we injected parental or catalase-deficient 231 cells into the tail vein of female nude mice and monitored tumor formation in the lungs over time (26). Intravenous injection was selected to force the 231 cells to grow in suspension as soon as they were injected into the animal. Following the injection of cells, we monitored the lungs of the mice every 2 weeks by X-ray CT scan (27). Over time, the lungs of the mice injected with parental 231 cells display dramatically less healthy lung volume (as measured by CT imaging) than do those of mice injected with catalase-deficient 231 cells (Fig. 6A and B). When animals were sacrificed 6 weeks following tail vein injection and their lungs were isolated, those injected with wild-type 231 cells had amassed substantial tumor burden on the lungs (Fig. 6C). However, the lung tumor burden in mice injected with catalase-deficient 231 cells was significantly reduced (Fig. 6C). Hematoxylin and eosin staining of the resulting tumors did not show any discernible differences in histology when comparing tumors from wild-type 231 cells to tumors from catalase-deficient 231 cells (Fig. 6C). We quantitated this effect by determining the percent of the lung tissue that contained tumor growth and found a statistically significant reduction in lung tumor burden in mice injected with catalase-deficient 231 cells (Fig. 6D). These data suggest that antioxidant enzymes are critical for the colonization of lung tissue by cancer cells through the promotion of ECM-detached cancer cell survival.

#### **Discussion**

The evasion of cell death by cancer cells, particularly during the metastatic cascade, has long been recognized as a hallmark of cancer (28). However, the precise mechanisms used by

Representative images are shown in D and quantitation of colony number is shown in E. Error bars represent SD and *P* values were determined using a 2-tailed *t* test. F, using lentiviral transduction of shRNA, catalase expression was reduced in T47D cells. Immunoblotting for catalase and  $\beta$ -actin (loading control) confirms the success of the transduction. G, ATP levels were measured under the indicated conditions after 24 hours of growth in suspension. Trolox treatment was at 50  $\mu$ mol/L. H and I, the indicated cells were grown in soft agar for 24 days and stained with INT-violet and counted using ImageJ. Trolox treatment was at 50  $\mu$ mol/L and applied every 2 days. Representative images are shown in H and quantitation of colony number is shown in I. Unless otherwise indicated, error bars represent SD and *P* values were determined using a 2-tailed *t* test.



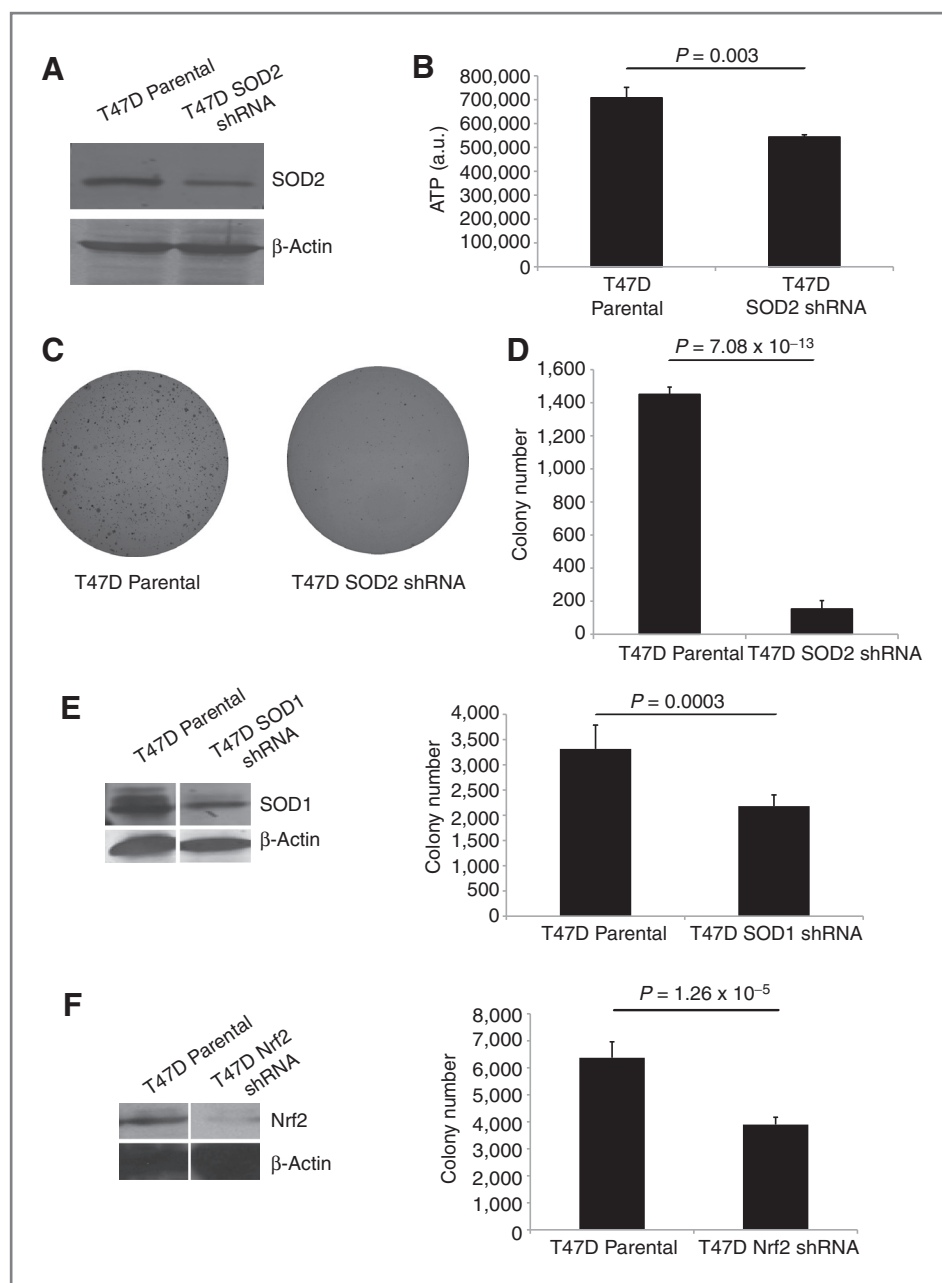


**Figure 5.** Other antioxidant enzymes can compromise ATP generation and anchorage-independent growth in cancer cells. A, using lentiviral transduction of shRNA, SOD2 expression was reduced in T47D cells. Immunoblotting for SOD2 and  $\beta$ -actin (loading control) confirms the success of the transduction. B, ATP levels were measured under the indicated conditions after 24 hours of growth in suspension. Error bars represent SD and  $P$  value was determined using 2-tailed  $t$  test. C and D, the indicated cells were grown in soft agar for 24 days and stained with iodonitrotetrazolium violet and counted using ImageJ. Representative images are shown in C and quantitation of colony number is shown in D. E, using lentiviral transduction of shRNA, SOD1 expression was reduced in T47D cells. Immunoblotting for SOD1 and  $\beta$ -actin (loading control) confirms the success of the transduction. The indicated cells were grown in soft agar for 16 days and stained with iodonitrotetrazolium violet and counted using Image J; quantitation of colony number is shown. Error bars represent SD, and  $P$  value was determined using a 2-tailed  $t$  test. F, using lentiviral transduction of shRNA, Nrf2 expression was reduced in T47D cells. Success of transduction was confirmed through immunoblotting for Nrf2 and  $\beta$ -actin (loading control). T47D and T47D Nrf2-deficient cells were grown in soft agar for 21 days and stained with iodonitrotetrazolium violet and counted using Image J; quantitation of colony number is shown. Error bars represent SD, and  $P$  value was determined using a 2-tailed  $t$  test.

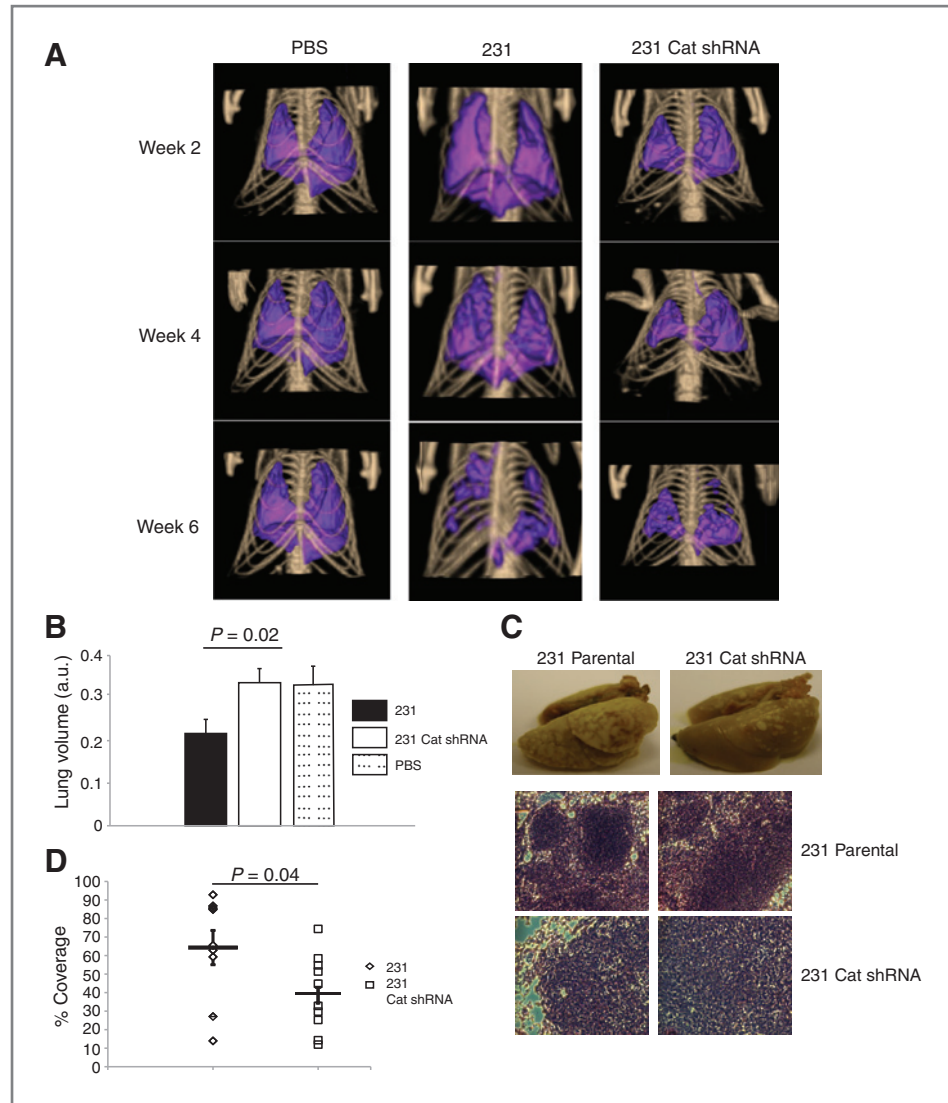
Downloaded from <http://aacrjournals.org/cancerresearch/article-pdf/73/1/237/042684589/3704.pdf> by guest on 28 March 2025

cancer cells to evade cell death caused by ECM-detachment have yet to be fully delineated. Here, using both *in vitro* and *in vivo* approaches, we describe a novel role for antioxidant enzymes in promoting the survival of ECM-detached breast cancer cells (see Fig. 7). The elimination of antioxidant enzymes has no discernible effect on the proliferation or survival of ECM-attached cancer cells, suggesting that the ability of antioxidant enzymes to facilitate cell survival is limited to ECM-detachment. Furthermore, these findings reveal a critical role for antioxidant enzymes in maintaining energy generation in ECM-detached cells and suggest that the specific elimination of antioxidant activity in ECM-detached

cancer cells may be an effective chemotherapeutic approach to halt metastatic spread.

Previously, we had shown that the treatment of MCF-10A cells with antioxidant compounds could rescue ECM-detachment induced ATP loss (10). The data reported here extend on these observations and reveal that enhanced expression of antioxidant enzymes can also elevate ATP levels in ECM-detached cells. The regulation of ATP generation by ROS seems to be due to the stimulation of AMPK activation when ROS levels are reduced. The precise mechanism by which AMPK levels are regulated by ROS remains poorly understood and will be the focus of future studies. In

**Figure 6.** Elimination of antioxidant enzyme expression reduces tumor formation *in vivo*. A, PBS, 231, or 231 catalase shRNA cells were injected ( $2 \times 10^6$  cells per injection) via tail vein into female nude mice. Representative CT images of lung volume were obtained at 2, 4, and 6 weeks after injection. B, quantitation of lung volume from CT scans at week 4 of 231, 231 catalase shRNA, and PBS injected mice ( $n = 6$  for PBS,  $n = 9$  for 231, and  $n = 10$  for 231 catalase shRNA). C, mice were sacrificed 6 weeks after injection and lungs were harvested and fixed in Bouin's solution. In addition, lungs were sectioned and stained with hematoxylin and eosin. Representative images of lungs from 231 and 231 catalase shRNA are shown. D, quantitation of lung tumor burden was conducted in mice that were injected with either 231 or 231 catalase shRNA cells ( $n = 9$  for 231 and  $n = 10$  for 231 catalase shRNA). Using ImageJ, the percentage of lung that was covered with tumor was quantified and plotted. All error bars represent SEM, and *P* values were determined using a 2-tailed *t* test.



addition, it is interesting to note that reduction in oxidative stress by multiple distinct mechanisms can similarly impact ATP generation in ECM-detached cells. For example, enzymes that neutralize peroxide (catalase), enzymes that eliminate superoxide (SOD2), and vitamin E analogs (Trolox) all have a strikingly similar capacity to elevate ATP levels in ECM-detached cells.

This study follows on the heels of other reports that emphasize the importance of neutralizing oxidative stress during tumor progression (29). Recently, it has become evident that the expression of a number of oncogenes (i.e., Ras, Raf, Myc) results in a reduction of oxidative stress that is dependent on the induction of Nrf2 (30). These data are consistent with the results reported here in that Nrf2, catalase, and SOD2 all have a similar capacity to promote ATP generation in ECM-detached cells. In addition, this report shows that Nrf2 is required for K-Ras (G12D)-mediated pancreatic tumor formation (30). Given our data, the loss of Nrf2 could result in a concomitant decrease

in the expression and activity of antioxidant enzymes thus rendering cancerous cells susceptible to cell death caused by ECM-detachment. Furthermore, recent work has revealed a critical role for pyruvate kinase M2 (PKM2) and CD44 in enhancing flux through the PPP, generating NADPH, and thus facilitating the survival of cancer cells during oxidative stress (31–33). In light of our data discussed here, it seems possible that cells expressing PKM2 and CD44 could be better equipped to handle deficiencies in antioxidant enzyme production to survive during ECM-detachment.

Another significant implication of the data presented here is the possibility that a reduction of antioxidant enzyme activity could be an attractive chemotherapeutic strategy for the specific elimination of ECM-detached cancer cells. Such a strategy could be particularly potent given that it has the potential to substantially inhibit the successful metastasis of cancer cells. Of course, additional studies must pursue the efficacy of inhibiting antioxidant

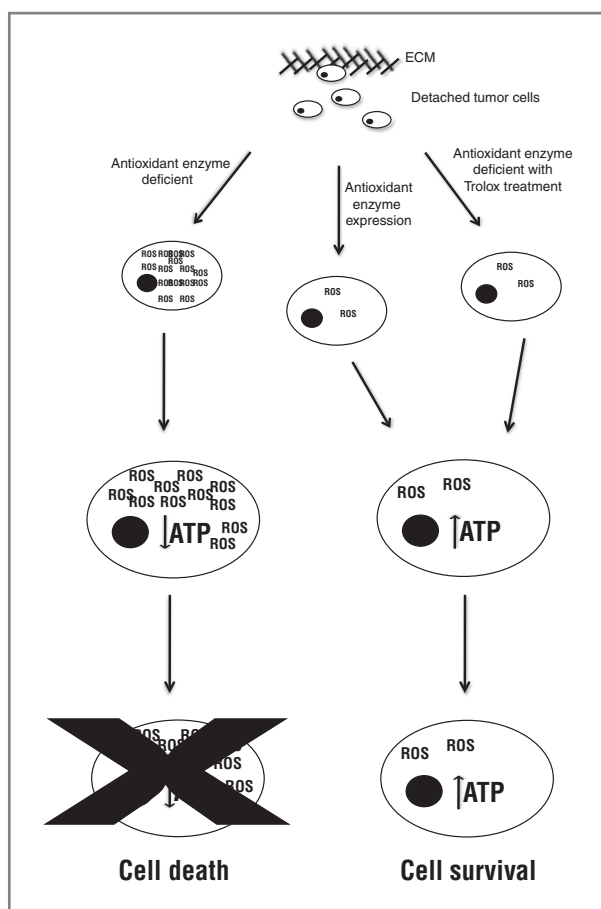


**Figure 7.** Model for antioxidant enzyme-mediated cell survival in ECM-detached breast cancer cells.

enzyme activity before any therapeutic development. For example, it is unclear whether the activity of antioxidant enzymes would similarly regulate the survival of ECM-detached cells in nonmammary cell types. Nonetheless, we

feel that the data presented here represent a significant advance in our understanding of how ECM-detached cancer cells survive and pave the way for future studies aimed at eliminating ECM-detached cancer cells through the modulation of antioxidant enzyme activity.

**Disclosure of Potential Conflicts of Interest**

No potential conflicts of interest were disclosed.

**Authors' Contributions**

**Conception and design:** C.A. Davison, M.R. Thau, Z.T. Schafer  
**Development of methodology:** C.A. Davison, M.R. Thau, S.E. Chapman, W.M. Leevy, Z.T. Schafer  
**Acquisition of data (provided animals, acquired and managed patients, provided facilities, etc.):** C.A. Davison, S. Durbin, V.R. Zellmer, S.E. Chapman, C. Wathen, W.M. Leevy  
**Analysis and interpretation of data (e.g., statistical analysis, biostatistics, computational analysis):** C.A. Davison, S. Durbin, S.E. Chapman, J. Diener, C. Wathen, W.M. Leevy, Z.T. Schafer  
**Writing, review, and/or revision of the manuscript:** C.A. Davison, M.R. Thau, S.E. Chapman, W.M. Leevy, Z.T. Schafer  
**Administrative, technical, or material support (i.e., reporting or organizing data, constructing databases):** C.A. Davison  
**Study supervision:** Z.T. Schafer

**Acknowledgments**

The authors thank Cassandra Buchheit, Raju Rayavarapu, Kelsey Weigel, Patricia Champion, Crislyn D'Souza-Schorey, Mark Suckow, Veronica Schafer, and the entire Schafer Lab for helpful comments, experimental assistance, and valuable discussion. The authors also thank Amy Leliaert for technical and organizational assistance and Stanley Terlecky (Wayne State University, Detroit, MI) for the gift of the catalase plasmids and Carestream Health for their assistance with the *in vivo* imaging approaches.

**Grant Support**

This work was supported by a V Scholar Award from the V Foundation for Cancer Research (Z.T. Schafer), by funds from the Coleman Foundation (Z.T. Schafer), by capitalization funds from the University of Notre Dame (Z.T. Schafer), and by a Notre Dame College of Science Summer Undergraduate Research Fellowship (M.R. Thau).

The costs of publication of this article were defrayed in part by the payment of page charges. This article must therefore be hereby marked *advertisement* in accordance with 18 U.S.C. Section 1734 solely to indicate this fact.

Received July 10, 2012; revised February 18, 2013; accepted March 20, 2013; published online June 14, 2013.

**References**

1. Frisch SM, Francis H. Disruption of epithelial cell-matrix interactions induces apoptosis. *J Cell Biol* 1994;124:619–26.
2. Frisch SM, Screaton RA. Anoikis mechanisms. *Curr Opin Cell Biol* 2001;13:555–62.
3. Taddei ML, Giannoni E, Fiaschi T, Chiarugi P. Anoikis: an emerging hallmark in health and diseases. *J Pathol* 2012;226:380–93.
4. Simpson CD, Anyiwe K, Schimmer AD. Anoikis resistance and tumor metastasis. *Cancer Lett* 2008;272:177–85.
5. Kim YN, Koo KH, Sung JY, Yun UJ, Kim H. Anoikis resistance: an essential prerequisite for tumor metastasis. *Int J Cell Biol* 2012;2012:306879.
6. Debnath J, Mills KR, Collins NL, Reginato MJ, Muthuswamy SK, Brugge JS. The role of apoptosis in creating and maintaining luminal space within normal and oncogene-expressing mammary acini. *Cell* 2002;111:29–40.
7. Overholtzer M, Mailleux AA, Mouneimne G, Normand G, Schnitt SJ, King RW, et al. A nonapoptotic cell death process, entosis, that occurs by cell-in-cell invasion. *Cell* 2007;131:966–79.
8. Florey O, Kim SE, Sandoval CP, Haynes CM, Overholtzer M. Autophagy machinery mediates macroendocytic processing and entotic cell death by targeting single membranes. *Nat Cell Biol* 2011;13:1335–43.
9. Fung C, Lock R, Gao S, Salas E, Debnath J. Induction of autophagy during extracellular matrix detachment promotes cell survival. *Mol Cell Biol* 2008;19:797–806.
10. Schafer ZT, Grassian AR, Song L, Jiang Z, Gerhart-Hines Z, Irie HY, et al. Antioxidant and oncogene rescue of metabolic defects caused by loss of matrix attachment. *Nature* 2009;461:109–13.
11. Buchheit CL, Rayavarapu R, Schafer ZT. The regulation of cancer cell death and metabolism by extracellular matrix attachment. *Semin Cell Dev Biol* 2012;23(4):402–11.
12. Zamocky M, Gasselhuber B, Furtmuller PG, Obinger C. Molecular evolution of hydrogen peroxide degrading enzymes. *Arch Biochem Biophys* 2012;525(2):131–44.
13. Zelko IN, Mariani TJ, Folz RJ. Superoxide dismutase multigene family: a comparison of the CuZn-SOD (SOD1), Mn-SOD (SOD2), and

- EC-SOD (SOD3) gene structures, evolution, and expression. *Free Radic Biol Med* 2002;33:337–49.
14. Thomas PA, Oykutlu D, Pou B, Tyler D, Oberley LW, Robinson RA, et al. Immunohistochemical characterization of antioxidant enzymes in human breast cancer. *Pathol Oncol Res* 1997;3:278–86.
  15. Somwar R, Erdjument-Bromage H, Larsson E, Shum D, Lockwood WW, Yang G, et al. Superoxide dismutase 1 (SOD1) is a target for a small molecule identified in a screen for inhibitors of the growth of lung adenocarcinoma cell lines. *Proc Natl Acad Sci U S A* 2011;108:16375–80.
  16. Mailleux AA, Overholtzer M, Schmelzle T, Bouillet P, Strasser A, Brugge JS. BIM regulates apoptosis during mammary ductal morphogenesis, and its absence reveals alternative cell death mechanisms. *Dev Cell* 2007;12:221–34.
  17. Debnath J, Muthuswamy SK, Brugge JS. Morphogenesis and oncogenesis of MCF-10A mammary epithelial acini grown in three-dimensional basement membrane cultures. *Methods* 2003;30:256–68.
  18. Aykin-Burns N, Ahmad IM, Zhu Y, Oberley LW, Spitz DR. Increased levels of superoxide and H<sub>2</sub>O<sub>2</sub> mediate the differential susceptibility of cancer cells versus normal cells to glucose deprivation. *Biochem J* 2009;418:29–37.
  19. Elangovan S, Ramachandran S, Venkatesan N, Ananth S, Gnana-Prakasam JP, Martin PM, et al. SIRT1 is essential for oncogenic signaling by estrogen/estrogen receptor alpha in breast cancer. *Cancer Res* 2011;71:6654–64.
  20. Koepke JI, Nakrieko KA, Wood CS, Boucher KK, Terlecky LJ, Walton PA, et al. Restoration of peroxisomal catalase import in a model of human cellular aging. *Traffic* 2007;8:1590–600.
  21. Yamada KM, Cukierman E. Modeling tissue morphogenesis and cancer in 3D. *Cell* 2007;130:601–10.
  22. Debnath J, Brugge JS. Modelling glandular epithelial cancers in three-dimensional cultures. *Nat Rev Cancer* 2005;5:675–88.
  23. Mills KR, Reginato M, Debnath J, Queenan B, Brugge JS. Tumor necrosis factor-related apoptosis-inducing ligand (TRAIL) is required for induction of autophagy during lumen formation in vitro. *Proc Natl Acad Sci U S A* 2004;101:3438–43.
  24. Reginato MJ, Mills KR, Becker EB, Lynch DK, Bonni A, Muthuswamy SK, et al. Bim regulation of lumen formation in cultured mammary epithelial acini is targeted by oncogenes. *Mol Cell Biol* 2005;25:4591–601.
  25. Reginato MJ, Mills KR, Paulus JK, Lynch DK, Sgroi DC, Debnath J, et al. Integrins and EGFR coordinately regulate the pro-apoptotic protein Bim to prevent anoikis. *Nat Cell Biol* 2003;5:733–40.
  26. Elkin M, Vlodaysky I. Tail vein assay of cancer metastasis. *Curr Protoc Cell Biol* 2001;Chapter 19:Unit 19 2.
  27. Davison CA, Chapman SE, Sasser TA, Wathen C, Diener J, Schafer ZT, et al. Multimodal optical, X-ray CT, and SPECT imaging of a mouse model of breast cancer lung metastasis. *Curr Mol Med* 2013.
  28. Hanahan D, Weinberg RA. Hallmarks of cancer: the next generation. *Cell* 2011;144:646–74.
  29. Poljsak B, Milisav I. The neglected significance of "antioxidative stress". *Oxid Med Cell Longev* 2012;2012:480895.
  30. DeNicola GM, Karreth FA, Humpton TJ, Gopinathan A, Wei C, Frese K, et al. Oncogene-induced Nrf2 transcription promotes ROS detoxification and tumorigenesis. *Nature* 2011;475:106–9.
  31. Anastasiou D, Poulgiannis G, Asara JM, Boxer MB, Jiang JK, Shen M, et al. Inhibition of pyruvate kinase M2 by reactive oxygen species contributes to cellular antioxidant responses. *Science* 2011;334:1278–83.
  32. Ishimoto T, Nagano O, Yae T, Tamada M, Motohara T, Oshima H, et al. CD44 variant regulates redox status in cancer cells by stabilizing the xCT subunit of system xc<sup>-</sup> and thereby promotes tumor growth. *Cancer Cell* 2011;19:387–400.
  33. Tamada M, Nagano O, Tateyama S, Ohmura M, Yae T, Ishimoto T, et al. Modulation of glucose metabolism by CD44 contributes to antioxidant status and drug resistance in cancer cells. *Cancer Res* 2012;72:1438–48.